ISTITUTO NAZIONALE DI FISICA NUCLEARE
Laboratori Nazionali di Frascati

LNF-83/22(R)
20 Aprile 1983

M. Enorini, M. Giammarchi, D. Menasce, D. Pedrini and A. Zallo:

A MONTECARLO PROGRAM FOR BEAUTY AND CHARM PHOTOPRODUCTION AT THE TEVATRON ENERGIES

Servizio Documentazione
dei Laboratori Nazionali di Frascati
Cas. Postale 13 - Frascati (Roma)

INFN - Laboratori Nazionali di Frascati
Servizio Documentazione

LNF-83/22(R)
20 Aprile 1983

A MONTECARLO PROGRAM FOR BEAUTY AND CHARM PHOTOPRODUCTION AT THE TEVATRON ENERGIES

M. Enorini, A. Zallo
INFN - Laboratori Nazionali di Frascati

M. Giammarchi, D. Menasce and D. Pedrini
Dipartimento di Fisica dell'Università di Milano, and INFN - Sezione di Milano

ABSTRACT.

A Montecarlo program is described which simulates the diffractive photoproduction of charm and beauty states for the vertex detector of the E 687 experiment at FNAL.

The program is now running on the Frascati and Milano VAX computers.

1. - INTRODUCTION.

In the search for beauty states two major points have to be considered: the signature of the candidates and the total sensitivity for beauty events.

These requests ask for a powerful vertex detector as identifier of beauty and charm decays. The matching of the vertex detector with a high resolution forward spectrometer reduces the high combinatorial background present in such processes. A vertex detector which uses a live target made of germanium and silicon solid state detectors has been recently proposed by a Frascati-Milano collaboration[1] to search for beauty and charm states in photoproduction at the Tevatron energies. A design of this vertex detector is given in Fig. 1.

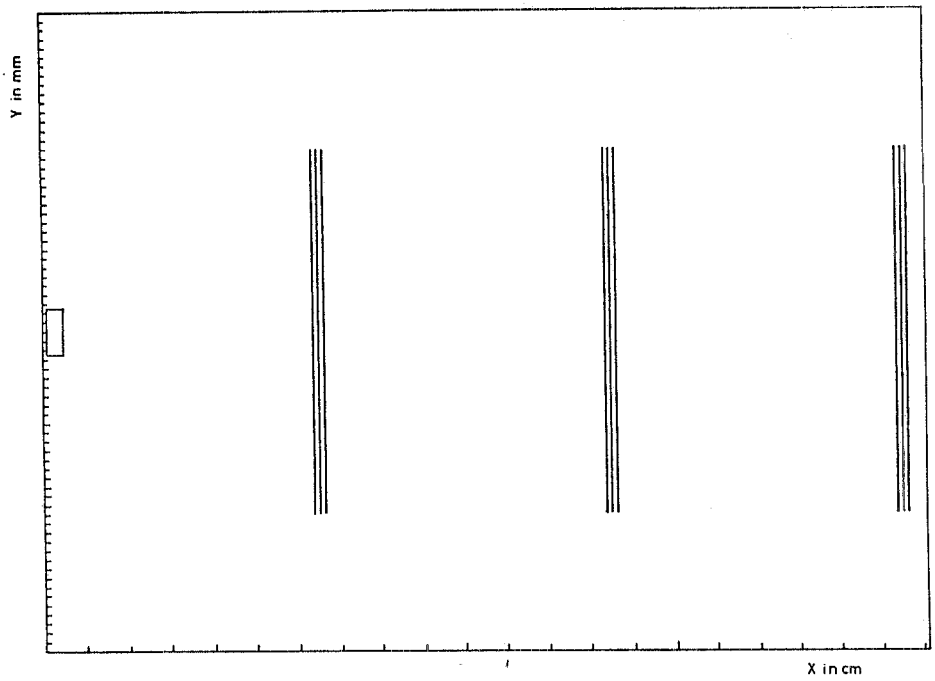

FIG. 1 - Vertex detector for E 687, the main detectors are: a) a Germanium target with 100 μm of pitch and a size of 2 cm in x, 0.5 cm in y and 0.4 cm in z; b) three sets of microstrips with 50 μm of pitch, a x,y size of 4 cm, positioned at 6 cm, 13 cm, 20 cm from the target.

In this report we describe a Montecarlo program that we have used to freeze the geometrical parameters of the proposed vertex detector and the granularity of the germanium detector.

The structure of the program is as follows:

- diffractive generation of beauty (charm) quarks;
- dressing of the quarks as physical particles following a Feynman, Field scheme[2];
- decay of the particles and their tracking through the vertex detector.

In Section 2 we give a brief description of the algorithms used for the generation and the dressing of the quarks and the decay of the particles.

The program can be run in an interactive way using a general purpose graphic package on Tektronix 4012.

It is in such a way possible to visualize the tracks and the vertex detector, change the granularity of the germanium or silicon detectors, change the geometry.

A full description of this graphic package and a list of instructions is given in Section 3.

Finally in Section 4 we give some results of the program as: displays of typical events, multiplicity distributions, minimum and maximum distance distributions.

2. - GENERATION AND DECAY OF BEAUTY AND CHARM PARTICLES.

The beauty-antibeauty, charm-anticharm particles have been generated according to the following steps :

a) Generation of a mass $M \div 1/M^2$.

b) Generation of the incoming photon with energy $E_\gamma \div 1/E_\gamma$; if the coherence of the nucleus is requested, the generation is a folding of a bremsstrahlung spectrum and the nucleus form factor. At this point we know the center of mass energy.

c) Generation of two quarks (b-$\bar{b}$) for beauties, (c-$\bar{c}$) for charms as the minimum quark content for the mass M. For the P_T distribution of these quarks we assume a diffractive production.

d) Dressing of the b-$\bar{b}$ (c-$\bar{c}$) quarks following algorithms similar to those used by the Lund group[3]. Quark-antiquark (q-$\bar{q}$) pairs are generated in their colour fields with a scaling function

$$Z = \frac{E + P_Z}{W_{PR}}$$

(E and P_Z are the energy and momentum along the jet axis of the q, W_{PR} is the same quantity for the primary quark) which defines the fraction of the energy and momentum carried by the quarks. The constraints from the energy and momentum conservation of the (q-$\bar{q}$) system are taken into account and the value of the mass M defines the number of extra-pions generated.

The decay of the particles is treated assuming the Kobayashi-Maskawa model[4] and the $b \rightarrow c$[5] dominance. Ali et al.[6] have calculated the relative probabilities for the different decay channels of Beauty particles. For the decay of the D mesons and the decay of the mesons which contain the ordinary quarks we use the branching ratios given in ref. (7).

3. - GRAPHIC PART DESCRIPTION.

A flow diagram of the program is shown in Fig. 2.

The structure is divided into three levels : initialization production and decays of particles, the graphic part. The interface between physics and displays is managed by the subroutine 'MENU' whose available options are:

'A' b-$\bar{b}$ event generation (by default).

'B' c-$\bar{c}$ event generation.

'D' diffractive event generation (by default).

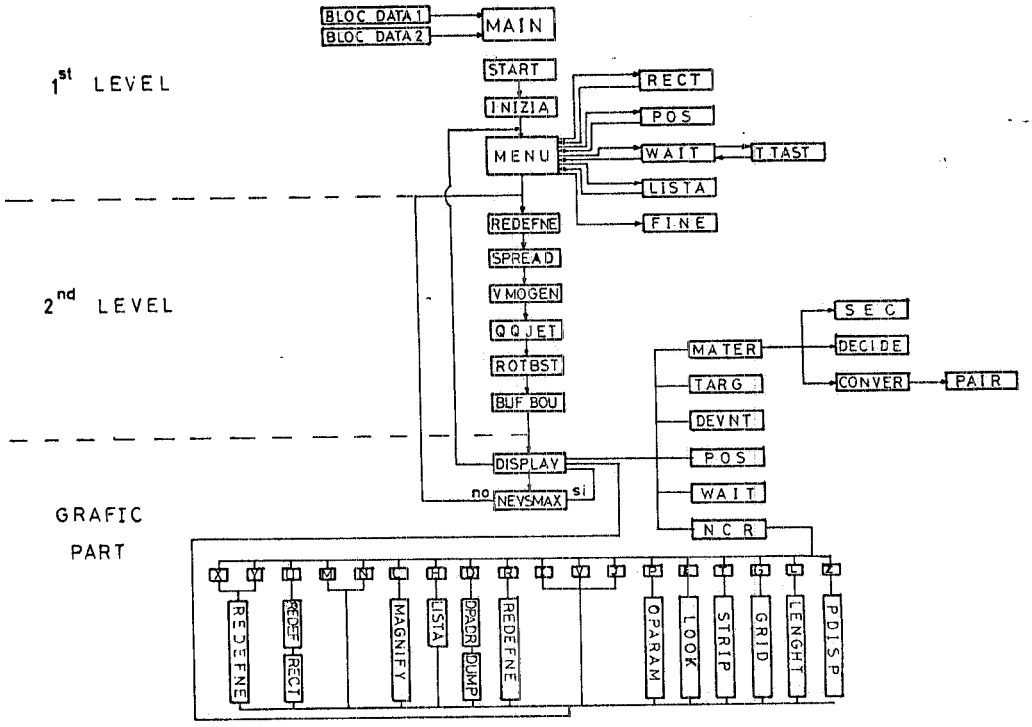

FIG. 2 - Flow diagram of the program.

'E' display of the last event progressive number, moreover the user can choose the number of the next event to be displayed. In such a way the computer can jump from one event to another without recording intermediate events.

'F' start of the program.

'G' stop of the program.

'H' list of available options in the graphic part.

'I' u-$\bar{u}$ event generation.

'L' d-$\bar{d}$ event generation.

'M' s-$\bar{s}$ event generation.

The real graphic part is connected to the other levels of the program only by the buffer that contains the physical information of the event, so this part can be easily connected to other programs. The program runs on a Tektronix 4012 graphic display with cursor facility connected to a VAX 11/780 computer; the subroutines use standard libraries (Packlib, Genlib, Kernlib, Teklib, Cvxlib) and a particular graphic library Mizar[8]. Except for the AST routine, written in macro-assembler, all the software is written in Fortran.

The subroutine 'Display' is responsible for the overall control of the various operations (see Fig. 2). We start with the geometrical tracking of the event and the

eventual gamma conversion in the layout of the experiment (see Fig. 3); then we arrive to the second set of available options. The user can choose the options by keyboard characters; in fact the AST (Asyncronous trap) routine stops the program waiting for the character. This ensures an asyncronous structure to the program.

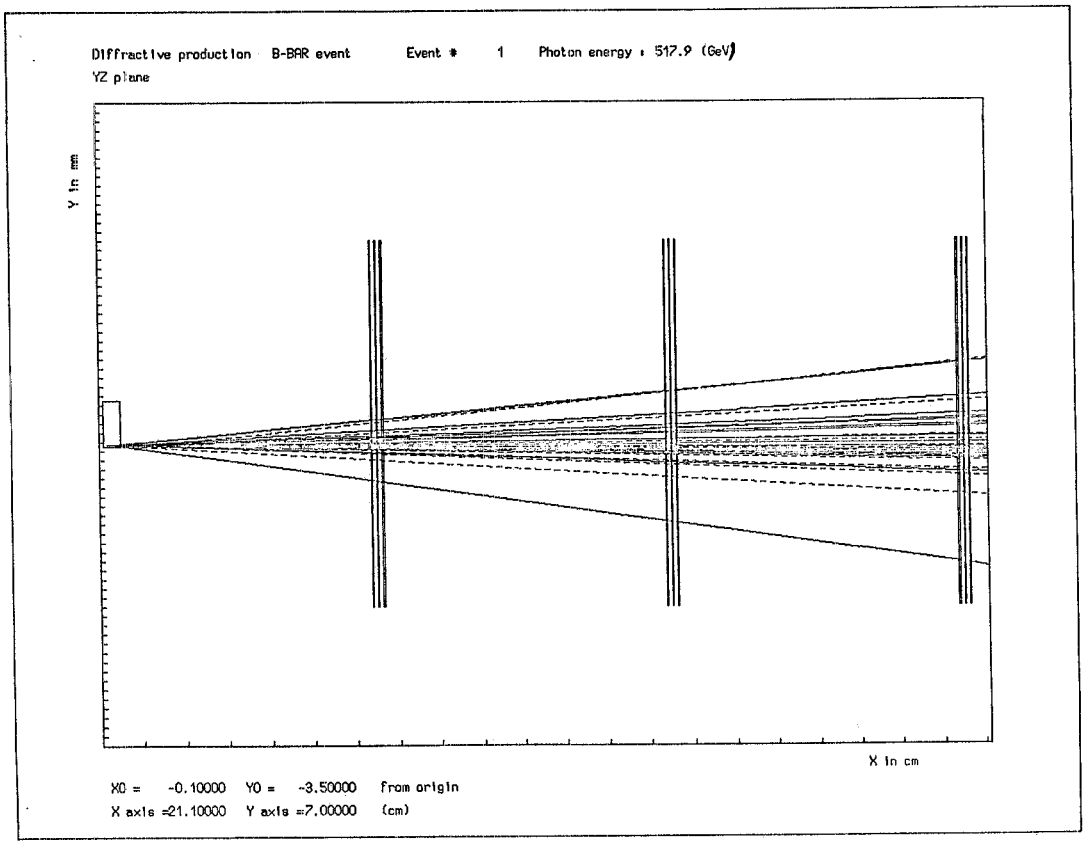

FIG. 3 - 1st event, side-view.

The available options are:

'X' event top-view, XZ plane (beam along Z-axis).

'Y' event side-view, YZ plane (by default).

'U' event perpendicular-view, XY plane.

'M' return to first level.

'N' display of next event.

'C' enlargement of an event sector, the user can choose the sectors by the cursors.

'H' display of available options with a short comment about the functions.

'D' display of event dump.

'R' restore normal view of display.

'I' display of neutral tracks (dash lines).

'V' display of charged tracks (by default).

'S' display of scale factors.

'P' changing of the most important physical parameters.

'E' display of particle character of a certain track; the user can choose the track by the cursors.

'T' display of the structure of the layers in the target and of the strip partition in the microstrips.

'G' display of the reference frame.

'L' display of the length between two points on the screen, the user can choose the points by the cursors.

'Z' recording of the picture seen on a file, to be printed eventually on paper.

The buffer, with which the graphic part interacts, has the following features: the first word gives the number of words in the buffer, then there are thirteen words for every particle; so (disregarding the first word) the buffer has a thirteen modular structure.

The thirteen words for every particle represent:

1. progressive number.
2. progressive number of the particle from which it comes from. If the particle comes from the primary vertex then the number is negative and represents quark composition according to Lund table[3].
3. particle code according to Lund table.
4.-7. Px, Py, Pz, E.
8.-10. x, y, z of production point.
11.-13. x, y, z of decay point.

A particle is assumed stable if it has a mean life greater than 10^{-10} s.

The most important aim of this graphic part is to display the events with all the details, to understand the differences between background and interesting events; moreover the enlargement of an event sector makes clear the decay chain.

4. - RESULTS.

We present in this last section some interesting results for the diffractive photoproduction of beauty and charm particles; the values of lifetimes assumed are:

$$\tau_B = 5 \times 10^{-14} \text{ s}, \qquad \tau_{D^0} = 4.8 \times 10^{-13} \text{ s}, \qquad \tau_{D^\pm} = 9.1 \times 10^{-13} \text{ s}.$$

In Figs. 4-10 we give some pictures of typical events. These events are presented with different enlargements which show the complex structure of the decay chains of the beauty and charm particles.

The multiplicity plots (see Fig. 11) have a mean value of ~ 6 at the end of the target, of ~ 10 at 3 cm from the target and of ~ 10 at the first set of microstrips. These plots show that most of the multiplicity jumps have a $Z \leq 3$ cm, so silicon detectors positioned in this region give a good signature of the decay chain of the beauty particles.

The minimum and maximum distances among the tracks fix the pitches and the sizes of the microstrips. The minimum distances, along x and y axis (see Fig. 12), show a mean value of $\sim 48\,\mu$m at the first set of microstrips, of $\sim 88\,\mu$m at the second one and of $\sim 113\,\mu$m at the third one. This results justify the choice of $50\,\mu$m as pitch of the microstrips.

The maximum distances (see Fig. 13) show a mean value of ~ 4.8 mm at the first set, of ~ 1 cm at the second one and of ~ 1.6 cm at the third one; this suggests a value of the trasversal dimension of the microstrips of about 4-5 cm.

These results agree with the geometrical values chosen for the vertex detector of E 687 collaboration[1], to which we refer for other results, as the reconstruction efficiencies.

REFERENCES.

(1) - Search on Beauty and Charm States using a Solid State Vertex Detector - E 687 Collaboration.

(2) - R. D. Field and R. P. Feynman, Nuclear Phys. B136, 1 (1978).

(3) - T. Sjöstrand, Lund Preprint LU TP 80-3 (1980).

(4) - M. Kobayashi and K. Maskawa, Prog. Theor. Phys. 49, 652 (1973).

(5) - C. Bebek et al., Phys. Rev. Letters 46, 84 (1981); K. Chadwick et al., Phys. Rev. Letters 46, 88 (1981).

(6) - A. Ali et al., Z. Physik C1, 203 (1979).

(7) - Particle Data Book (1982).

(8) - Private communication by A. Giorgilli (Dipartimento di Fisica dell'Università di Milano).

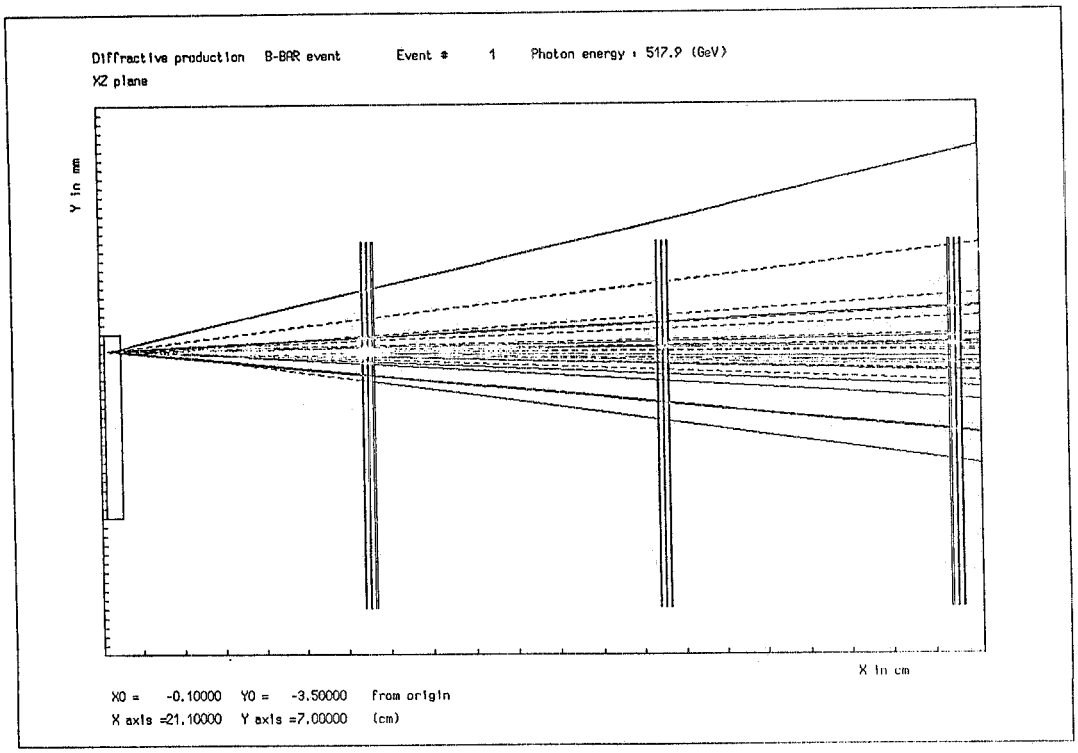

FIG. 4 - 1st event, top-view.

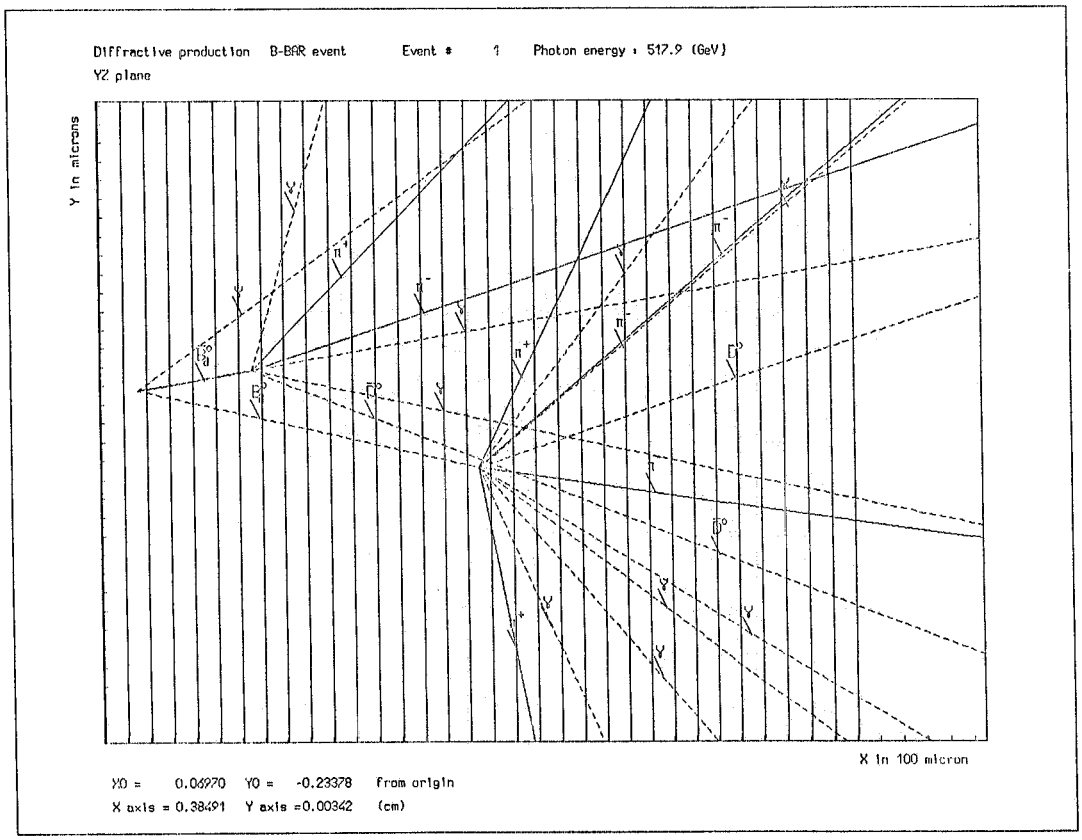

FIG. 5 - Enlargement of a target sector, 1st event.

Diffractive production Event # 1 Photon energy :517.9 (GeV)

#	From	Type	XPRO	YPRO	ZPRO	XDEC	YDEC	ZDEC
1.	-26.	B_d^{0*}	0.81841	-0.23190	0.08639	0.81841	-0.23190	0.08639
2.	-11.	$\bar{B}_d^{0*}$	0.81841	-0.23190	0.08639	0.81841	-0.23190	0.08639
3.	1.	B_d^0	0.81841	-0.23190	0.08639	0.81843	-0.23232	0.23478
4.	1.	ν	0.81841	-0.23190	0.08639	0.80471	-0.22911	0.39572
5.	2.	$\bar{B}_d^0$	0.81841	-0.23190	0.08639	0.81841	-0.23180	0.13580
6.	2.	ν	0.81841	-0.23190	0.08639	Stable	Stable	Stable
7.	3.	ρ^+	0.81843	-0.23232	0.23478	0.81843	-0.23232	0.23478
8.	3.	D^{0*}	0.81843	-0.23232	0.23478	0.81843	-0.23232	0.23478
9.	3.	ρ^-	0.81843	-0.23232	0.23478	0.81843	-0.23232	0.23478
10.	3.	ρ^0	0.81843	-0.23232	0.23478	0.81843	-0.23232	0.23478
11.	5.	π^+	0.81841	-0.23180	0.13580	Stable	Stable	Stable
12.	5.	ρ^-	0.81841	-0.23180	0.13580	0.81841	-0.23180	0.13580
13.	5.	$\bar{D}^0$	0.81841	-0.23180	0.13580	0.81217	-0.23613	1.04447
14.	7.	π^+	0.81843	-0.23232	0.23478	Stable	Stable	Stable
15.	7.	π^0	0.81843	-0.23232	0.23478	0.81844	-0.23232	0.23502
16.	8.	D^0	0.81843	-0.23232	0.23478	0.81435	-0.22805	1.26662
17.	8.	π^0	0.81843	-0.23232	0.23478	0.81843	-0.23232	0.23480
18.	9.	π^-	0.81843	-0.23232	0.23478	Stable	Stable	Stable
19.	9.	π^0	0.81843	-0.23232	0.23478	0.81844	-0.23232	0.23531
20.	10.	π^+	0.81843	-0.23232	0.23478	Stable	Stable	Stable
21.	10.	π^-	0.81843	-0.23232	0.23478	Stable	Stable	Stable
22.	12.	π^-	0.81841	-0.23180	0.13580	Stable	Stable	Stable
23.	12.	π^0	0.81841	-0.23180	0.13580	0.81842	-0.23180	0.13588
24.	13.	K^0	0.81217	-0.23613	1.04447	0.81217	-0.23613	1.04447
25.	13.	ω	0.81217	-0.23613	1.04447	0.81217	-0.23613	1.04447
26.	13.	π^0	0.81217	-0.23613	1.04447	0.81215	-0.23613	1.04499
27.	15.	ν	0.81844	-0.23232	0.23502	Stable	Stable	Stable
28.	15.	ν	0.81844	-0.23232	0.23502	Stable	Stable	Stable
29.	16.	ω	0.81435	-0.22805	1.26662	0.81435	-0.22805	1.26662
30.	16.	$\bar{K}^{0*}$	0.81435	-0.22805	1.26662	0.81435	-0.22805	1.26662
31.	17.	ν	0.81843	-0.23232	0.23480	0.81881	-0.22983	0.39076
32.	17.	ν	0.81843	-0.23232	0.23480	Stable	Stable	Stable
33.	19.	ν	0.81844	-0.23232	0.23531	Stable	Stable	Stable
34.	19.	ν	0.81844	-0.23232	0.23531	Stable	Stable	Stable
35.	23.	ν	0.81842	-0.23180	0.13588	Stable	Stable	Stable
36.	23.	ν	0.81842	-0.23180	0.13588	0.83475	-0.22513	0.29013
37.	24.	K_s^0	0.81217	-0.23613	1.04447	0.75162	-0.51545	203.30467
38.	25.	π^+	0.81217	-0.23613	1.04447	Stable	Stable	Stable
39.	25.	π^-	0.81217	-0.23613	1.04447	Stable	Stable	Stable
40.	25.	π^0	0.81217	-0.23613	1.04447	0.81216	-0.23614	1.04522
41.	26.	ν	0.81215	-0.23613	1.04499	Stable	Stable	Stable
42.	26.	ν	0.81215	-0.23613	1.04499	0.48513	-0.31821	6.25794
43.	29.	π^+	0.81435	-0.22805	1.26662	Stable	Stable	Stable
44.	29.	π^-	0.81435	-0.22805	1.26662	Stable	Stable	Stable
45.	29.	π^0	0.81435	-0.22805	1.26662	0.81435	-0.22805	1.26672
46.	30.	K^-	0.81435	-0.22805	1.26662	Stable	Stable	Stable
47.	30.	π^+	0.81435	-0.22805	1.26662	Stable	Stable	Stable
48.	37.	π^+	0.75162	-0.51545	203.30467	Stable	Stable	Stable
49.	37.	π^-	0.75162	-0.51545	203.30467	Stable	Stable	Stable
50.	40.	ν	0.81216	-0.23614	1.04522	Stable	Stable	Stable
51.	40.	ν	0.81216	-0.23614	1.04522	Stable	Stable	Stable
52.	45.	ν	0.81435	-0.22805	1.26672	Stable	Stable	Stable
53.	45.	ν	0.81435	-0.22805	1.26672	Stable	Stable	Stable
100.	4.	e^-	0.80471	-0.22911	0.39572	Stable	Stable	Stable
101.	4.	e^+	0.80471	-0.22911	0.39572	Stable	Stable	Stable
102.	31.	e^-	0.81881	-0.22983	0.39076	Stable	Stable	Stable
103.	31.	e^+	0.81881	-0.22983	0.39076	Stable	Stable	Stable
104.	36.	e^-	0.83475	-0.22513	0.29013	Stable	Stable	Stable
105.	36.	e^+	0.83475	-0.22513	0.29013	Stable	Stable	Stable
106.	42.	e^-	0.48513	-0.31821	6.25794	Stable	Stable	Stable
107.	42.	e^+	0.48513	-0.31821	6.25794	Stable	Stable	Stable

FIG. 6 - Dump of 1st event.

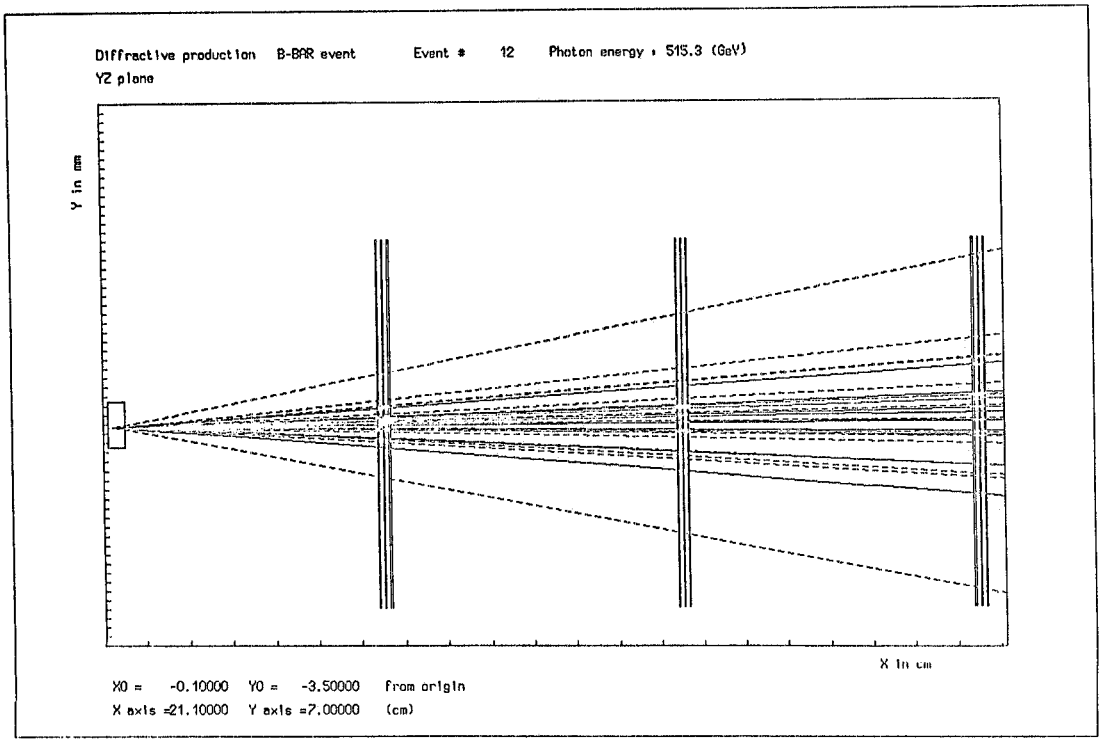

FIG. 7 - Another typical event: 12 th event, side view.

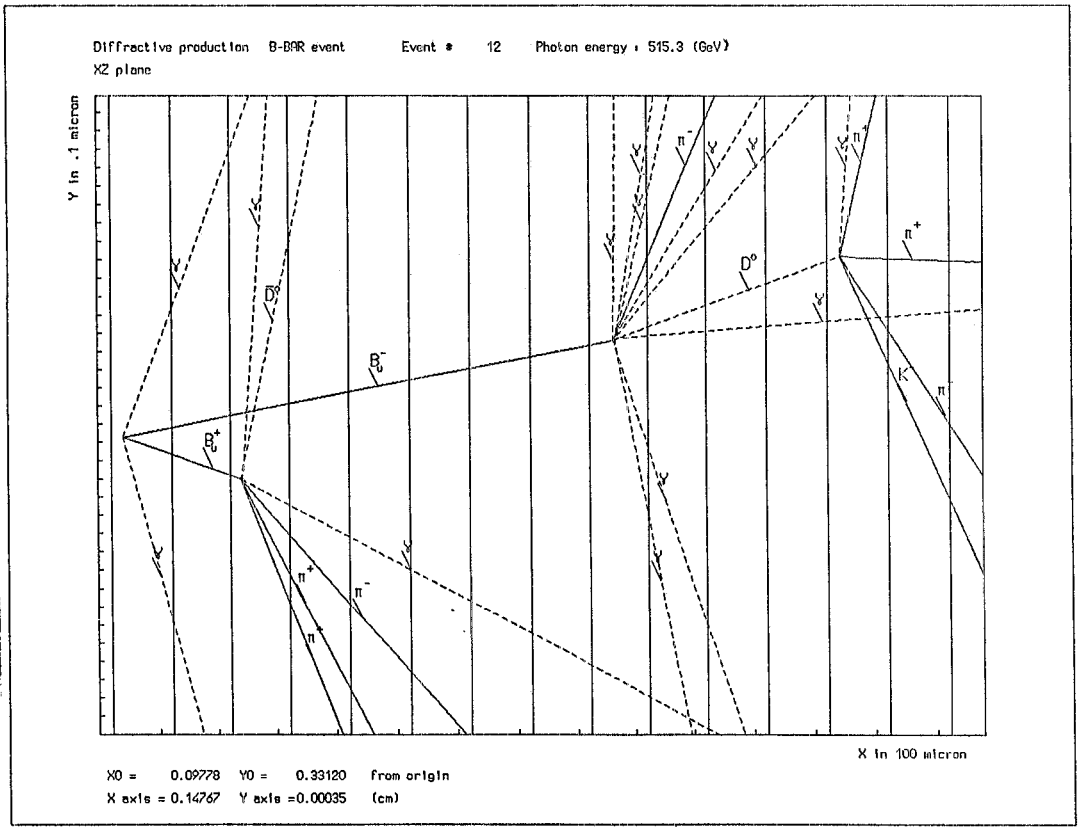

FIG. 8 - Enlargement of a target sector, 12th event.

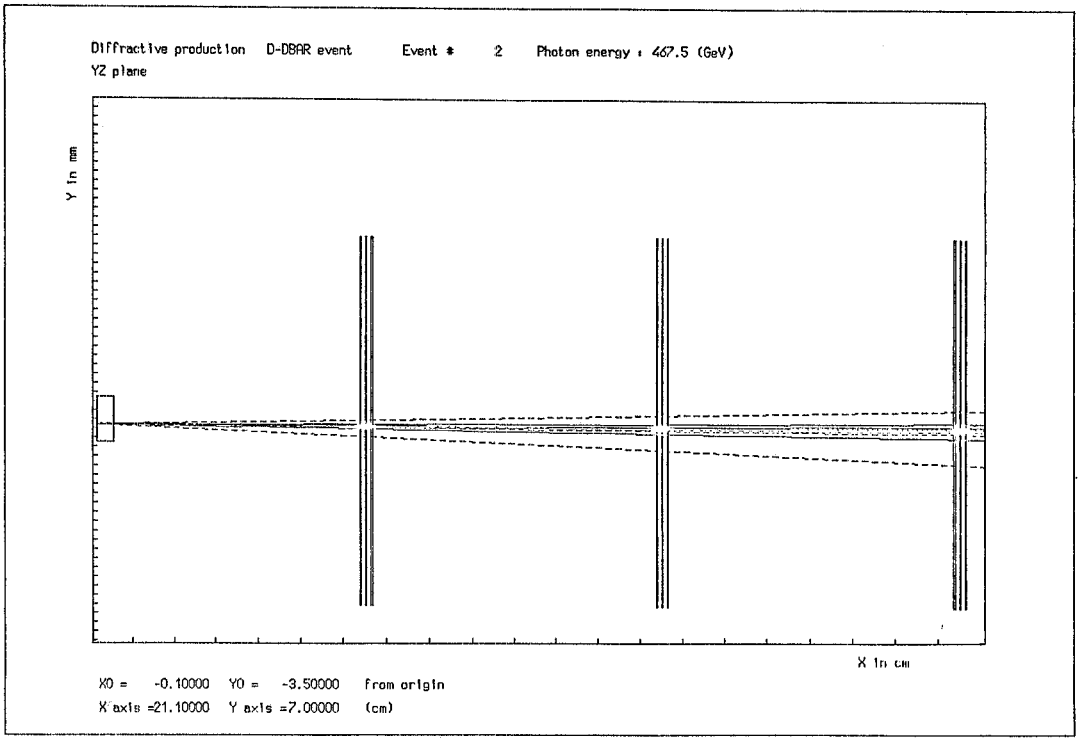

FIG. 9 - A D-$\bar{D}$ event : 2nd event, side view.

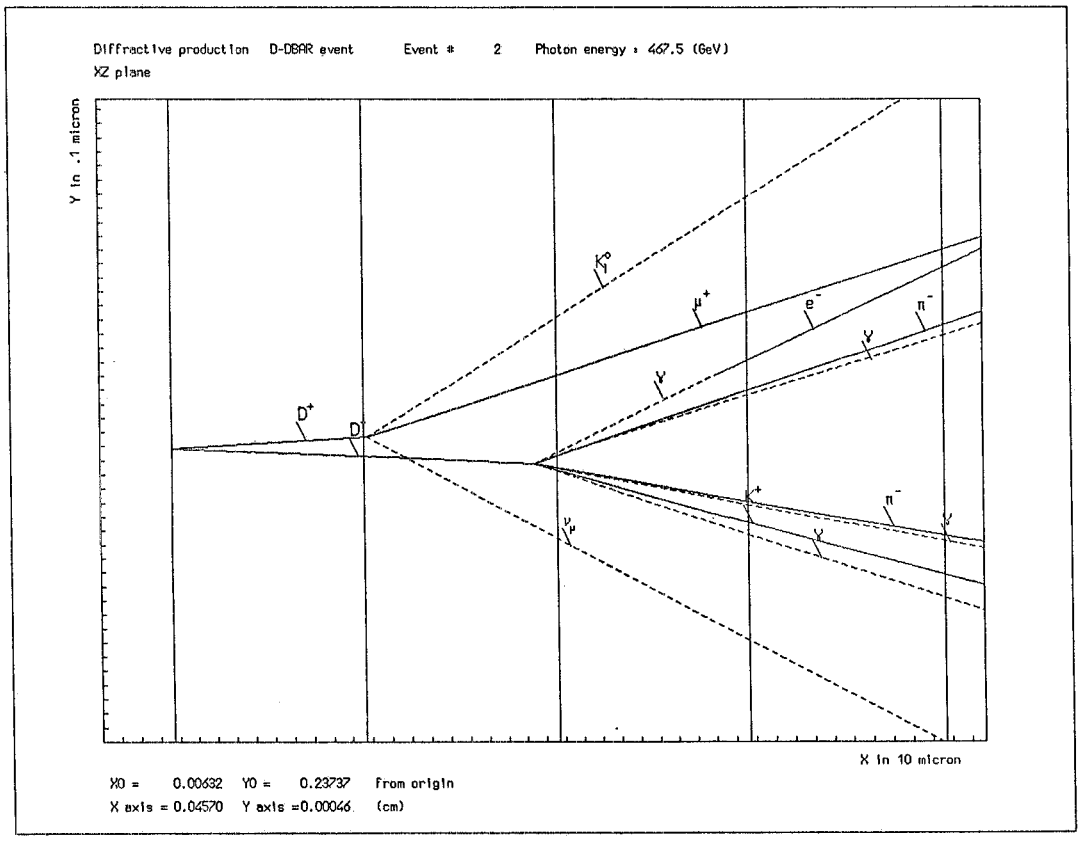

FIG. 10 - Enlargement of a target sector, 2nd event.

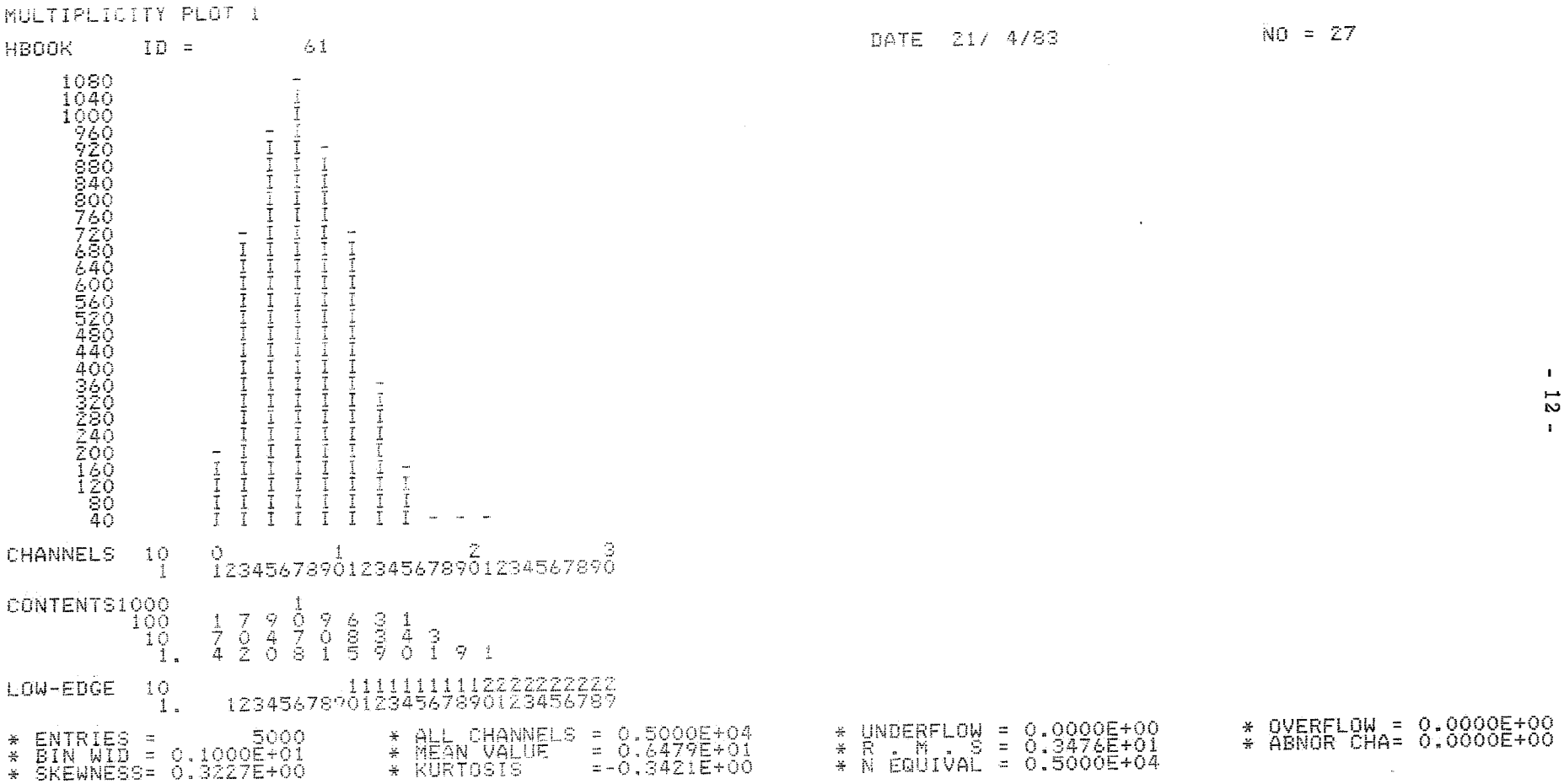

FIG. 11a) - Multiplicity plots, at the end of the target.

FIG. 11b) - Multiplicity plots, at 3 cm from the target.

FIG. 11c) - Multiplicity plots, at the first set of microstrips.

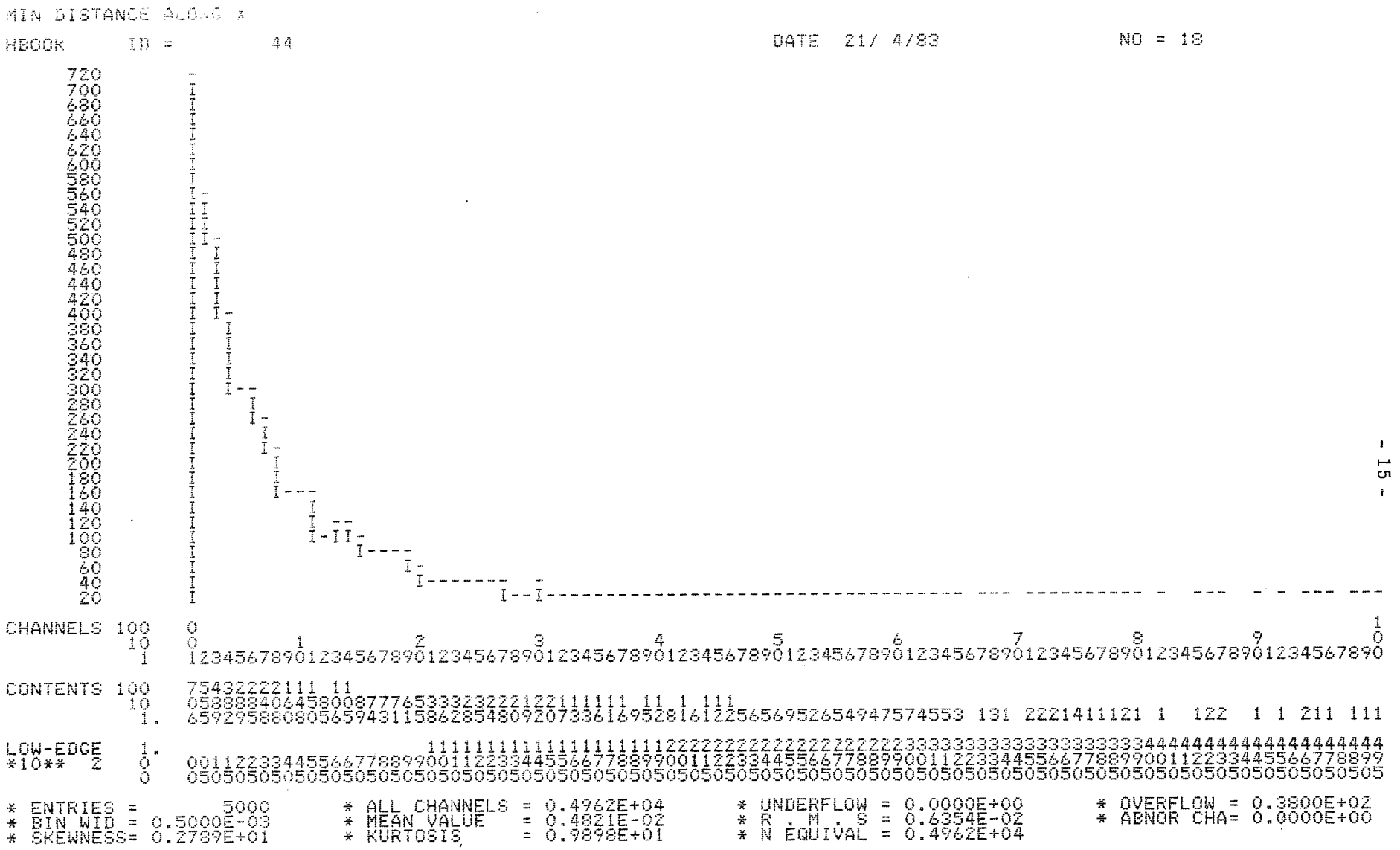

* ENTRIES = 5000 * ALL CHANNELS = 0.4962E+04 * UNDERFLOW = 0.0000E+00 * OVERFLOW = 0.3800E+02
* BIN WID = 0.5000E-03 * MEAN VALUE = 0.4821E-02 * R . M . S = 0.6354E-02 * ABNOR CHA= 0.0000E+00
* SKEWNESS= 0.2789E+01 * KURTOSIS = 0.9898E+01 * N EQUIVAL = 0.4962E+04

FIG. 12a) - Minimum distance distributions (in cm).

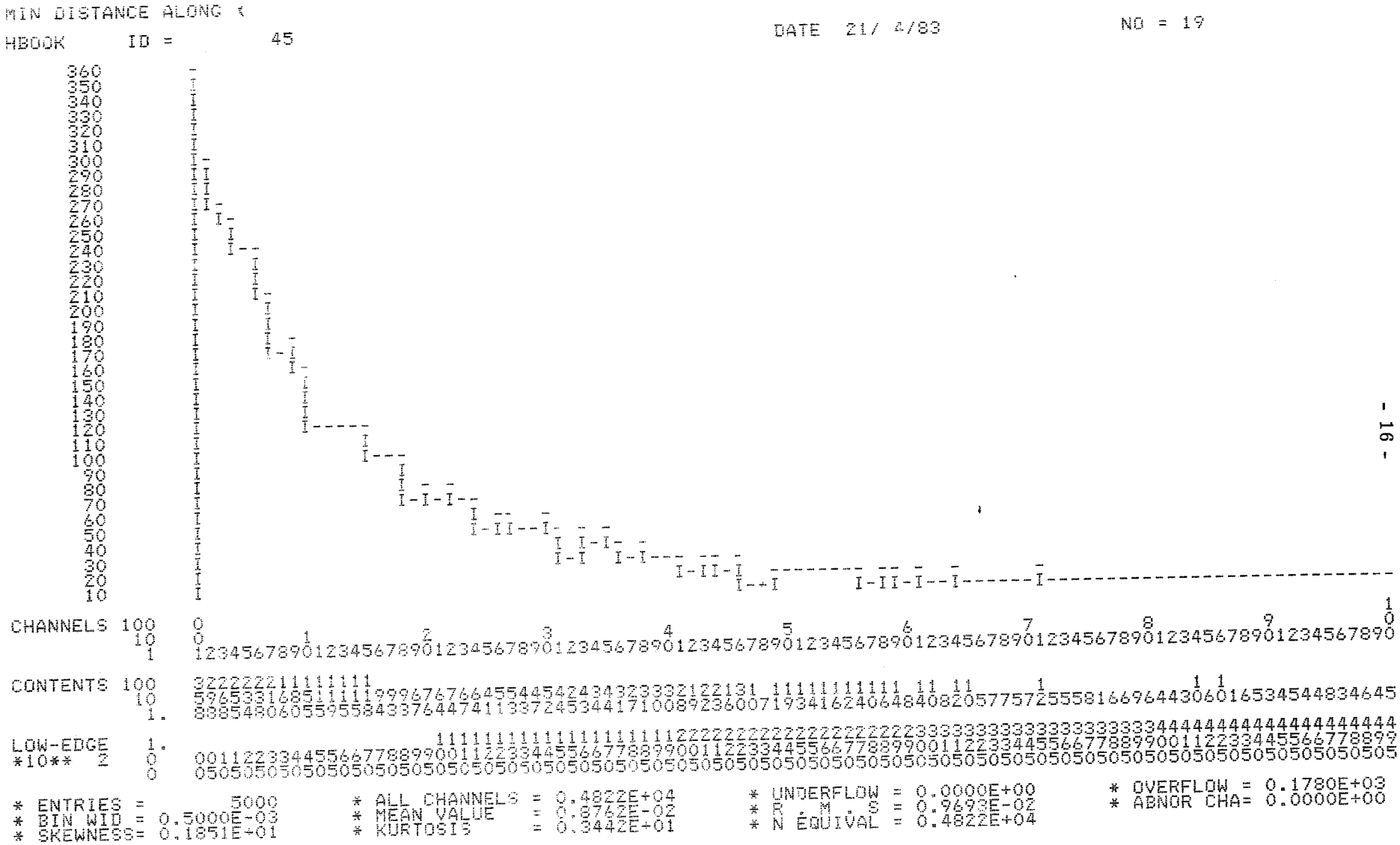

FIG. 12b) - Minimum distance distributions (in cm).

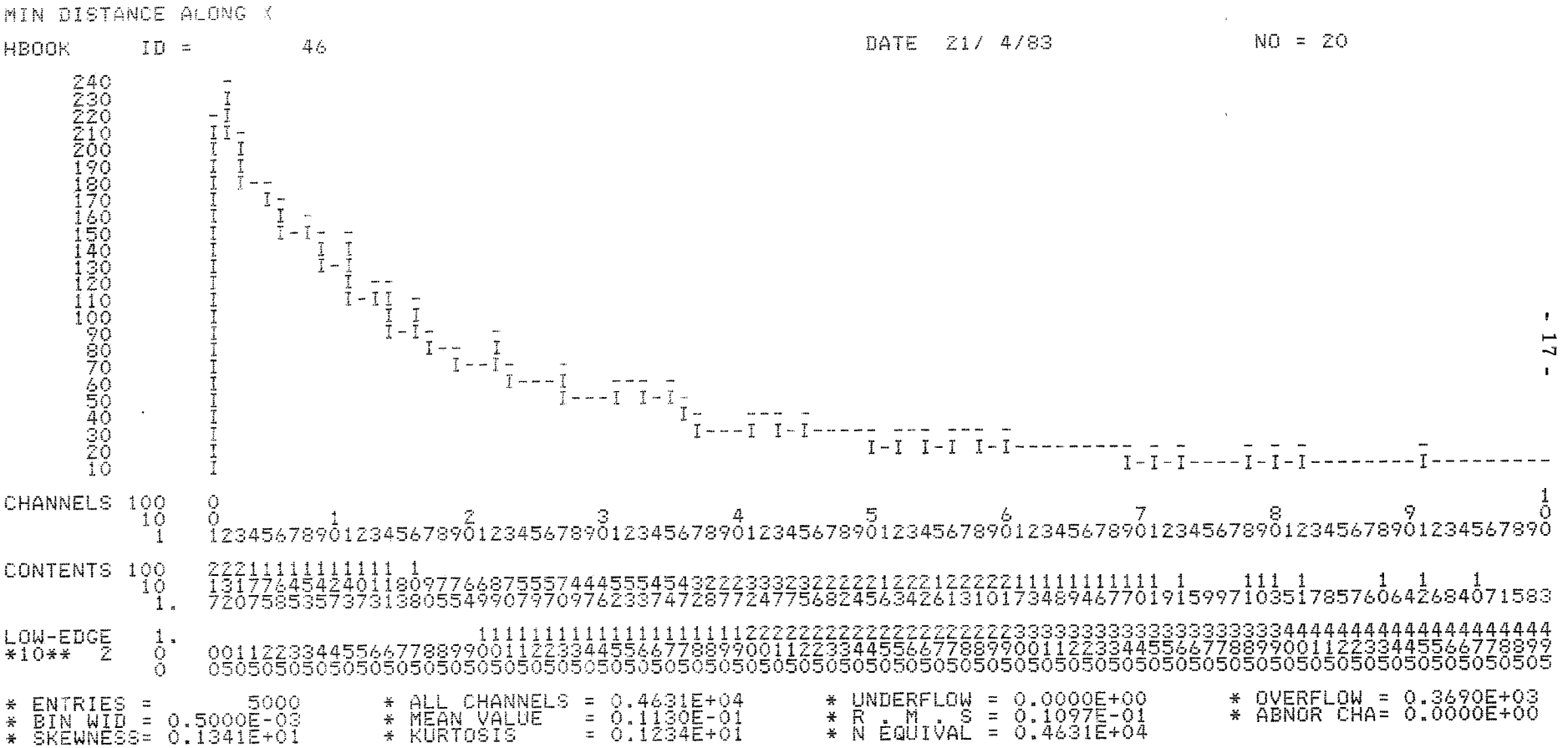

FIG. 12 c) - Minimum distance distributions (in cm).

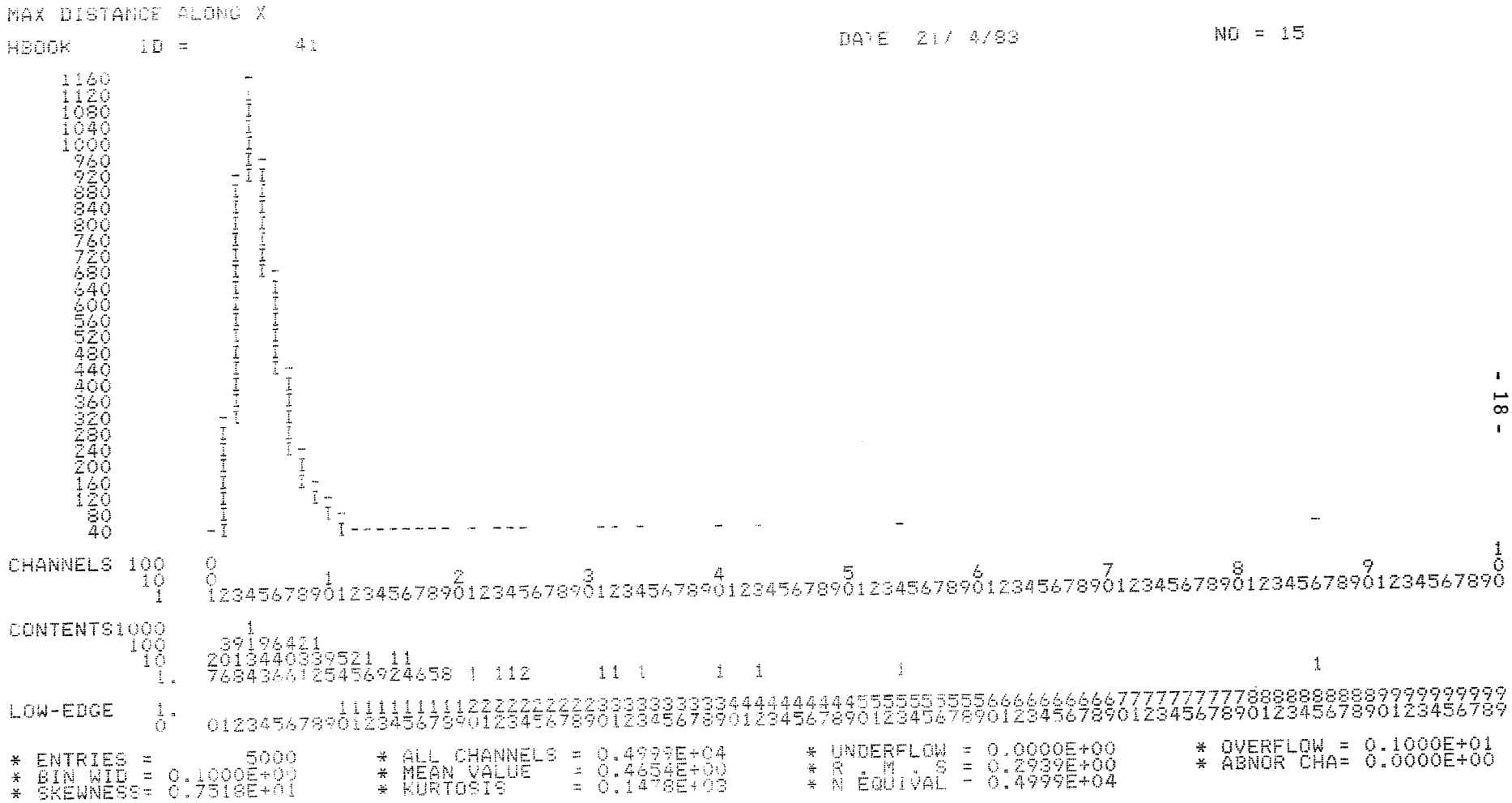

FIG. 13 a) - Maximum distance distributions (in cm).

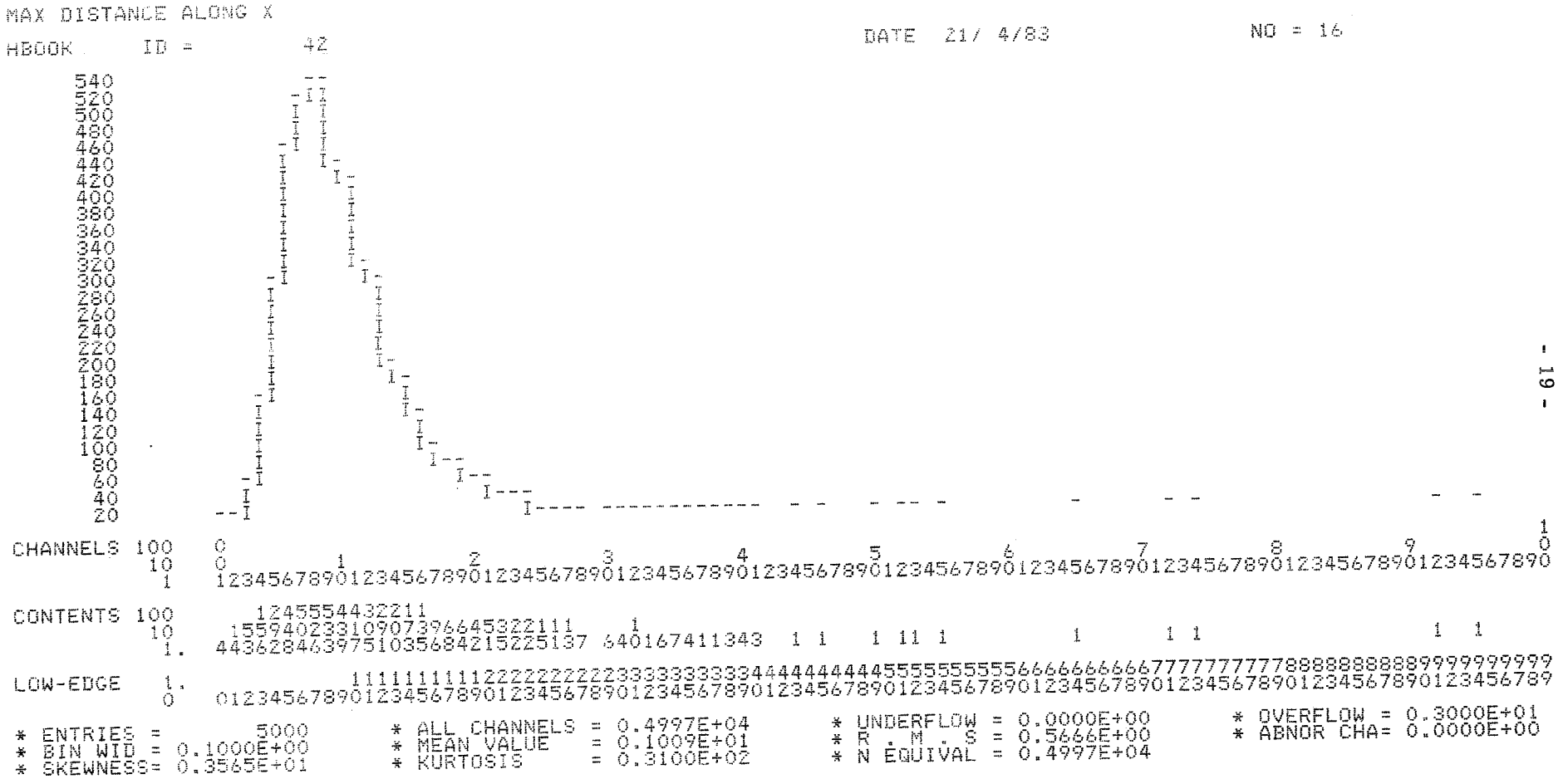

FIG. 13 b) - Maximum distance distributions (in cm).

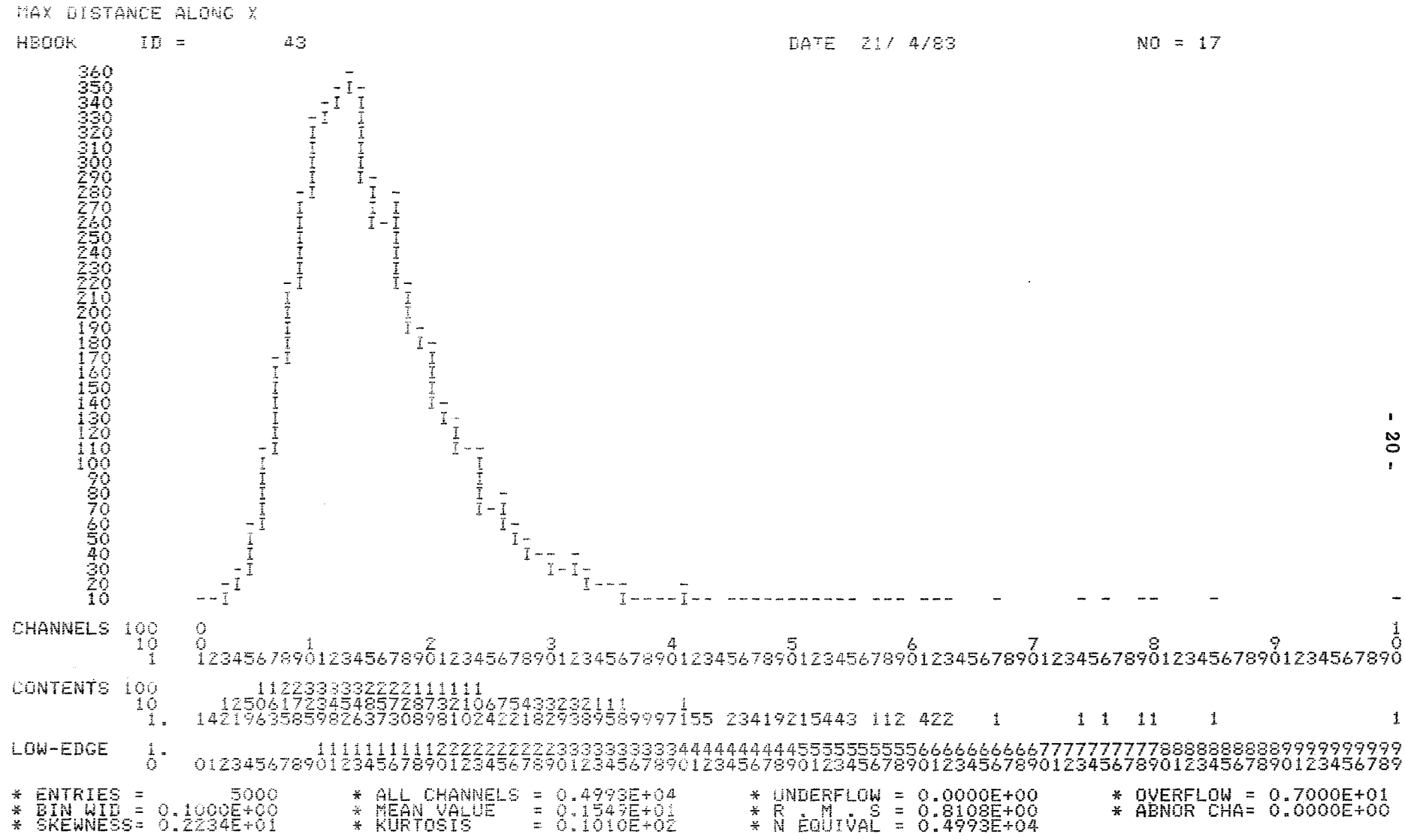

FIG. 13 c) - Maximum distance distributions (in cm).